

Isotopes in Environmental and Health Studies



ISSN: (Print) (Online) Journal homepage: www.tandfonline.com/journals/gieh20

A protocol for distilling animal body water from biological samples and measuring oxygen and hydrogen stable isotopes via cavity ring-down spectroscopy

Zachary T. Steele, Karen Caceres, Austin D. Jameson, Michael Griego, Elizabeth J. Rogers & John P. Whiteman

To cite this article: Zachary T. Steele, Karen Caceres, Austin D. Jameson, Michael Griego, Elizabeth J. Rogers & John P. Whiteman (12 Mar 2024): A protocol for distilling animal body water from biological samples and measuring oxygen and hydrogen stable isotopes via cavity ring-down spectroscopy, Isotopes in Environmental and Health Studies, DOI: 10.1080/10256016.2024.2323201

To link to this article: https://doi.org/10.1080/10256016.2024.2323201





METHOD



A protocol for distilling animal body water from biological samples and measuring oxygen and hydrogen stable isotopes via cavity ring-down spectroscopy

Zachary T. Steele^a, Karen Caceres^a, Austin D. Jameson^a, Michael Griego^a, Elizabeth J. Rogers^b and John P. Whiteman^a

^aDepartment of Biological Sciences, Old Dominion University, Norfolk, VA, USA; ^bOrganismic & Evolutionary Biology Program, University of Massachusetts, Amherst, MA, USA

ABSTRACT

The application of stable isotope analysis (SIA) to the fields of ecology and animal biology has rapidly expanded over the past three decades, particularly with regards to water analysis. SIA now provides the opportunity to monitor migration patterns, examine food webs, and assess habitat changes in current and past study systems. While carbon and nitrogen SIA of biological samples have become common, analyses of oxygen or hydrogen are used more sparingly despite their promising utility for tracing water sources and animal metabolism. Common ecological applications of oxygen or hydrogen SIA require injecting enriched isotope tracers. As such, methods for processing and analyzing biological samples are tailored for enriched tracer techniques, which require lower precision than other techniques given the large signal-to-noise ratio of the data. However, instrumentation advancements are creating new opportunities to expand the applications of high-throughput oxygen and hydrogen SIA. To support these applications, we update methods to distill and measure water derived from biological samples with consistent precision equal to, or better than, $\pm 0.1 \%$ for δ^{17} O, $\pm 0.3 \%$ for δ^{18} O, ± 1 % for δ^{2} H, ± 2 % for d-excess, and ± 15 per meg for Δ^{17} O.

ARTICLE HISTORY

Received 30 June 2023 Accepted 1 February 2024

KEYWORDS

Cryogenic; doubly labeled water; hydrogen-2; isotope ecology; metabolic water; oxygen-17 excess; oxygen-18; Picarro; plasma; triple oxygen isotopes

1. Introduction

Stable isotope analysis (SIA) is a powerful tool that has been increasingly incorporated into ecology and animal biology [1–3]. Many studies of animal tissues focus on nitrogen and carbon stable isotopes (δ^{15} N and δ^{13} C; [1,4]), which can support inferences regarding an animal's diet and role in a food web [5], migration patterns [6], and even paleoecology [7]. Stable isotopes of oxygen and hydrogen (δ^{18} O and δ^{2} H) can provide information related to the sources of environmental water intake and to the animal's body water pool [8,9]. For example, measurements of injected 2 H and 18 O tracers can reflect the size of the body water pool and the metabolic rate [10,11], natural abundance of 18 O can reflect environmental water sources [12,13], and a new application that

simultaneously measures natural abundance of 16 O, 17 O, and 18 O (i.e. Δ^{17} O) can be used to infer relative changes in metabolic rate and water intake [9,14,15]. Most hydrogen and oxygen analyses use blood plasma or serum samples [11], but under the right circumstances (e.g. a trained animal in captivity) saliva and urine samples can be collected as well [16]. A central premise for all these methods is that water is critical to animal biology [17]. Most terrestrial animals are $\sim 60-70\,\%$ water by mass, and this body water comes from a combination of environmental sources (i.e. ingestion of preformed water by drinking or eating) and endogenous processes (e.g. newly-synthesized metabolic water, a byproduct of metabolic pathways; [13,18]). Despite the utility of hydrogen and oxygen SIA to many ecological applications, these isotopes are generally applied less often in animal biology than carbon and nitrogen stable isotopes, in part because of the difficulty involved in processing and analyzing samples [8].

To analyze body water, it must first be distilled out of tissue [11]. For example, blood plasma is ~ 90 % water by mass, with the remainder including organic (e.g. proteins) and inorganic (e.g. electrolytes) components which could damage instruments and interfere with isotope measurements [17]. Typically, cryogenic vacuum distillation is used for distilling body water samples [19,20], and most researchers rely on the methods description in Wood et al. [21] or Nagy [22] for this method. Over the last decade (2013–2023), 59 % of publications (53 of 90; identified via Google Scholar) involving the distillation of animal plasma samples cited these two sources for their distillation methods or Speakman [11], which summarizes the work of Nagy [22]. In the Nagy [22] method, a microcapillary tube containing a biological sample such as plasma is broken into segments that are placed into the large end of a glass Pasteur pipette. The large opening of the pipette is then flame sealed. The narrow end of the pipette is then connected to a vacuum pump; the larger end of the pipette is dipped into liquid nitrogen (LN₂) until the plasma samples are solidly frozen; then a vacuum is applied before the narrow end is quickly flame sealed. The sample remains frozen, sealed in a vacuum. The larger end of the pipette is then placed on a slide warmer, with the narrow end extending off the edge of the slide warmer. As the sample thaws and the tissue water evaporates, it eventually condenses at the narrow end because of the cooler temperatures off the edge of the slide warmer, while non-volatile components of the tissue (e.g. proteins) remain in the larger end. A final flame seal is then used to isolate the narrow end, leaving a makeshift microcapillary tube of distilled body water.

While the distillation approach described by Nagy [22] can be generically applied to any sample containing water, the publication was written as a guide for doubly labeled water (DLW) studies. The DLW technique is a prominent approach to estimating the metabolism of both captive and free-ranging animals [11]. The DLW method relies on using isotope tracers that are significantly enriched with heavy isotopes of hydrogen (typically 2H but occasionally 3H is still used) and oxygen (almost exclusively ^{18}O), resulting in δ values that can be \geq 1000 % for 2H and ^{18}O [11]. When studying free-ranging animals, the DLW method typically begins with an initial capture event and the collection of a blood sample [11]. The animal is then injected with the enriched isotope tracers, and after allowing time for the injected isotopes to reach equilibration with the animal's body water, a second sample is taken [11]. After the equilibration sampling, the animal is released and returns to normal activity in their environment. Lastly, the animal is recaptured after a predetermined timeframe dependent on their body water turnover rate to

collect a final sample [11]. By comparing this final sample with the equilibration sample, the rate of elimination of the oxygen and hydrogen isotopes can be used to estimate CO₂ production and thus metabolic rate [11]. The estimation of CO₂ production is possible because oxygen isotopes will be expelled in both water and CO₂, while hydrogen isotopes will only be lost in water, allowing for back-calculation of CO2 production because the heavy oxygen isotope 'label' is associated with both H₂O and CO₂ flux rates [11].

In Nagy's [22] guide, the author recommended measuring stable isotopes of hydrogen via liquid scintillation counting (using ³H), and of oxygen via proton activation of ¹⁸O to ¹⁸F followed by counting ¹⁸F in a gamma counter. These measurement approaches were recommended over isotope ratio mass spectrometry (IRMS) despite having lower accuracy and precision because of the labor and expenses related to IRMS, which is still a relevant issue today [11,22]. The scintillation and gamma counting recommended by Nagy [22] require substantial enrichment of oxygen and hydrogen tracers, which is compatible with the DLW technique. DLW and other enriched isotope tracer techniques generally require less accuracy and precision to generate viable data compared to natural abundance analyses because the range of measurements is so vast (i.e. natural abundance measurements of ¹⁸O in precipitation generally fall between -25 and 10 ‰, whereas measurements may span > 1000 ‰ in a DLW study). This reduced need for precision in enriched studies is important because recent technological advancements have dramatically expanded the realm of natural abundance isotope studies.

While IRMS remains a fixture, cavity ring-down spectroscopy (CRDS) and off-axis integrated cavity output spectroscopy (OA-ICOS) offer new, more affordable alternatives that provide rapid and often automated measurement of hydrogen and oxygen isotopes [23,24], CRDS and OA-ICOS can measure both δ^{17} O and δ^{18} O simultaneously with the precision required for calculating Δ^{17} O, which is the residual in the near-linear relationship between δ^{17} O and δ^{18} O. This residual reflects mass-independent fractionation because the slope of the relationship reflects mass-dependent fractionation [25,26]. While the framework for calculating $\Delta^{17}O$ has been understood for \sim 50 years [27], interest in Δ^{17} O has rapidly expanded in the last ~ 25 years, particularly in paleoclimatology, geochemistry, and hydrology [25,28–30]. In addition, Δ^{17} O has recently been applied to animal samples in ecological and physiological studies [9,14,15,31-34]. The two primary sources of water for animals - preformed (drinking/food water) and metabolic water are expected to have unique and relatively consistent Δ^{17} O values of 41 per meg (parts per million) and -441 per meg, respectively [9,35]. Considering that these two sources typically constitute $\sim 80-99 \,\%$ of an animal's body water [13], $\Delta^{17}O_{BW}$ (measured $\Delta^{17}O$ in body water) can provide insight about the contribution of metabolic water and therefore metabolism as well [9,34].

Calculation of Δ^{17} O requires highly precise and accurate measurement of δ^{17} O and δ^{18} O with measurement errors \leq 0.015 ‰, and all 2 H- and 18 O-based analyses require that sample preparation avoids fractionation, which would bias results. This increased need for precision and accuracy, and the recently increased scope of applications, necessitates revisiting previous methods for sample distillation such as those discussed in Nagy [22]. Our aim in writing this manuscript is to support the expansion of SIA of oxygen and hydrogen, particularly by: (1) researchers who currently analyze solid biological materials (e.g. fossilized teeth), but not liquid materials; (2) ecologists and animal biologists currently sending their samples for SIA at other institutes, interested in submitting liquid

samples; and (3) ecologists and animal biologists who are interested in oxygen and hydrogen SIA, but who view the high costs and complex procedures as barriers. As such, we thoroughly detail methods related to sample processing and analysis for a broad audience, with the goal of being accessible to non-isotope specialists. We describe distillation of blood plasma and analysis via CRDS, although our methods can be used for distilling a variety of samples (e.g. urine or saliva) and using any isotope instrumentation.

2. Overview of $\Delta^{17}O_{BW}$ and potential applications of measurements

When measurements of both $\delta^{17}O$ and $\delta^{18}O$ are obtained, $\Delta^{17}O$ is calculated as follows [26]:

$$\Delta^{17}O = \delta'^{17}O - 0.528 \cdot \delta'^{18}O \tag{1}$$

The 'symbol indicates linearization via the following equation using δ^{18} O as an example:

$$\delta'^{18}O = ln(\delta^{18}O + 1)$$
 (2)

Without this linearization, the relationship between $\delta^{17}O$ and $\delta^{18}O$ would be curved. When measurements of $\delta'^{17}O$ and $\delta'^{18}O$ are plotted against each other, a near constant and predictable relationship is observed (hence the slope of 0.528 applied in Equation (1) [26]). This relationship occurs because the isotope variation of $\delta^{17}O$ and $\delta^{18}O$ is typically based on mass (i.e. via mass-dependent fractionation) and means that a sample with a high $\delta^{18}O$ value is expected to also have a high $\delta^{17}O$ value. However, there are small positive and negative deviations from this expected relationship, representing mass-independent fractionation which are quantified as $\Delta^{17}O$ [36].

Interest in Δ^{17} O analyses of atmospheric oxygen has increased in the last two decades because of its potential as a tool for understanding hydrological cycles and reconstructing paleoclimates from samples such as ice cores [37,38]. Other studies have measured Δ^{17} O in animal bones because atmospheric oxygen becomes incorporated into animal tissue during aerobic metabolism [14,32]. These studies expanded upon physiological models built to predict δ^{18} O in animal tissues for similar paleoclimate reconstruction [12,13]. More recently, measurements of Δ^{17} O in animal tissues have been placed into an ecophysiological perspective and proposed as a tool to model animal metabolism and water intake [9]. Animal biology applications of Δ^{17} O are limited thus far but interesting modern and paleo results have been obtained from captive and free-ranging avian species [15,34], elasmobranchs and cetaceans [33], bovids and cervids [9,14,31], small rodents [9,14], and ursids [9]. Importantly, the relevant scale of Δ^{17} O values is approximately two orders of magnitude smaller than the scale for the underlying measurements of δ^{18} O and δ^{17} O. For example, in our experience with ecophysiological applications, δ^{18} O variation of 20 ‰ is commonly encountered (e.g. range of -15 to 5 ‰) with corresponding Δ^{17} O variation of < 0.200 ‰ (i.e. < 200 per meg).

Regardless of whether Δ^{17} O is interpreted in the context of paleoclimatology, ecophysiology, or other fields, modeling the drivers of Δ^{17} O is complicated. For example, highly-evaporated plant water can have a uniquely negative Δ^{17} O value [39–42], a potentially confounding influence when attempting to assess animal metabolism of an herbivore based on the input of atmospheric oxygen, which also has a strongly negative Δ^{17} O value [32]. This confounding influence can be potentially accounted for using updated

isotope modeling techniques, and with complementary data (e.g. δ^2 H, d-excess which is calculated from δ^{18} O and δ^{2} H) that can simultaneously be measured via CRDS or OA-ICOS [32]. For example, plant waters with uniquely negative Δ^{17} O values may also have unique δ^2 H signatures that help to differentiate between the influence of atmospheric oxygen and plant waters [39,43,44]. Importantly, measurement error can limit the application of modeling techniques and reduce the accuracy of complementary isotope measurements. Therefore, highly precise and accurate measurements of stable oxygen and hydrogen isotopes are needed for three distinct reasons: (1) to enable calculation of Δ^{17} O; (2) for related measurements (e.g. δ^{18} O, δ^{2} H, and d-excess) that provide additional information for interpreting Δ^{17} O; and (3) to enable interpretation of oxygen fluxes (e.g. drinking water, metabolic water, exhalation of carbon dioxide) via isotope modeling techniques [32]. Since unintended fractionation during sample preparation (e.g. distillation errors) should be mass-dependent, such fractionation should bias values of δ^{18} O and δ^{17} O simultaneously, while not altering Δ^{17} O. Consequently, trends among δ^{18} O, δ^{17} O, and Δ^{17} O could accidentally become dissociated during sample preparation, emphasizing the need for precision and accuracy.

Most studies applying Δ^{17} O measurements to animals have utilized samples from solid materials such as tooth enamel [14,31,33]. While these studies have greatly expanded the understanding of Δ^{17} O, they are limited to the use of physical chemistry (e.g. fluorination) for sample preparation followed by IRMS and they tend to focus on long-term averages of physiological parameters (e.g. average metabolic rate during the time of tooth enamel formation; [45,46]). In contrast, Δ^{17} O from distilled plasma samples [9,15] can reflect short time periods (e.g. the days to weeks required for body water turnover; [45,46]) and can be measured via CRDS or OA-ICOS.

3. Distilling body water from blood plasma samples

Herein, we describe the process of distilling a blood plasma sample to obtain a body water sample for isotope analysis. A complete video tutorial of the entire process is included as Video S1 and can be downloaded via Github or accessed via YouTube (please see Supplementary materials).

A single distillation following the process described below typically requires an initial volume of blood plasma of 35 –125 μL to yield enough volume for CRDS analysis. For example, a 2 mL sample of blood plasma yields ~ 55 separate distillations, providing ample opportunities to replicate measurements of the sample. Once the desired volume for a single distillation is selected, insert this volume into the large end of a glass pipette (for a full list of recommended materials for the distillation process see Table 1). Nagy [22] described filling a microcapillary tube with sample, then breaking that tube into small sections and inserting the sections into the glass pipette with forceps. However, these sections are susceptible to shattering when freezing in LN₂ during later steps, and they may trap residual sample during distillation. Instead, we recommend that sample be transferred directly into the large end of the glass pipette via a micropipette unless working with small sample volumes (< 20 µL); this approach requires careful handling of the pipette because the liquid plasma can easily shift position during the next step.

Once the sample has been inserted into the glass pipette, flame seal the larger end (in Figure 1A, the 'larger opening' at Point A) of the pipette with a micro-torch. This step

Table 1. List of required and optional materials for completion of the distillation process. Recommended brands and product numbers are included when relevant (if not a '—' is placed in this column).

Item description	Recommended brand and product number	Purpose		
9" Borosilicate glass Pasteur pipettes	Kimble 883350-0009	Vessel for the distillation process		
Butane micro-torch and butane fuel	Bernzomatic Butane Micro Torch ST2200T	Flame sealing glass pipette		
Cylindrical form dewar flasks	Pope Scientific 8645 (1000 mL) or 8621 (1900 mL)	Holding LN ₂ or dry ice		
Slide warmer	C&A Scientific Premiere Slide Warmer XH-2001	Warming pipettes to transfer distilled body water to narrow end of pipette		
Forceps	_	Gripping glass pipette for flame sealing		
Sharpening stone	-	Breaking down glass pipettes or microcapillary tubes		
Vacuum Pump	Vacuubrand ME1 20721000	Creating vacuum seal after dipping pipette into LN_2 or dry ice		
Microcapillary tubes (optional)	=	(Depending on method) For inserting sample into glass pipette		
Micropipette and pipette tips (optional)	-	(Depending on method) For inserting sample into glass pipette		

should first be practiced with empty pipettes then with pipettes containing tap water before handling samples. It is important to balance the glass pipette horizontally, ensuring the sample remains in the body of the pipette (Figure 1A, Point C) and does not flow toward the narrow opening (Figure 1A, Points D and E) or toward the indented transition point (Figure 1A, Point B). We recommend placing the micro-torch on a stable surface and locking the flame on (with appropriate precautions) to allow the use of both hands for the pipette and forceps. Flame sealing is completed by grasping the pipette at Point D with one hand and then positioning the flame near the larger opening of the pipette, and slowly rolling the pipette back and forth. The hand that is not holding the pipette should be holding the forceps. The flame should be applied roughly a third of the distance from the larger opening toward the indented transition point (see Figure 1A). Rotate the pipette slowly and fully so that the seal is complete. The glass will soften after ~ 20 s and at that moment, use the forceps to grasp the side of the larger opening of the pipette and gently pull away; the glass should move freely and leave a small, thin trail attached to the pipette. To complete this seal, gently move this trail through the flame for several seconds until the trail melts down into a small button shape.

The appearance of flame seals falls into three general categories: good seals have a button-shaped end that sits nicely on the closed glass-end; average seals are more jagged and extend outwards from the glass but still have a button-shaped end; and bad seals have no button or even an obvious gap in the seal (Figure 1B). When a good seal is completed properly, a flame seal should not result in any fractionation to the sample (Table 2). While the difference between a good and average seal may seem trivial, an average seal is more likely to cause the glass pipette to shatter later in the process, and it increases the likelihood of incomplete distillation in which body water remains trapped at the larger end of the pipette at the end of the process. This incomplete distillation presents the greatest threat of undesired fractionation and imprecise, biased data. Incomplete distillations due to trapped sample is not mentioned by Nagy [22], likely because the alteration of the δ^{18} O values was insignificant to the desired outcomes.

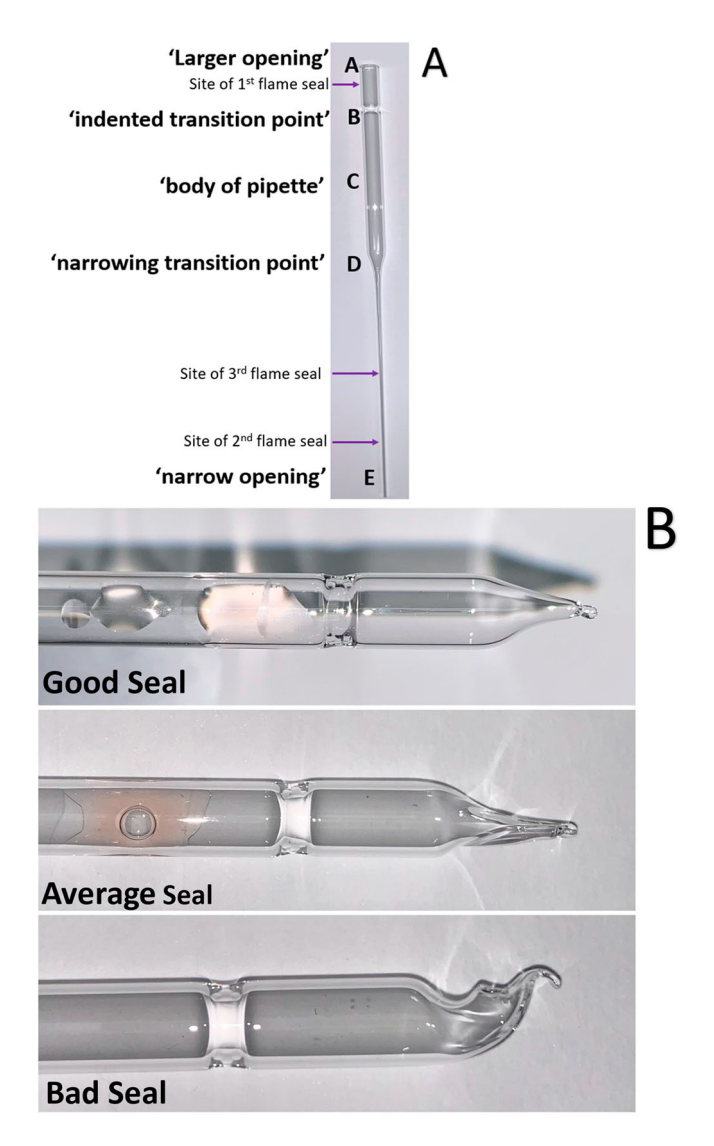


Figure 1. A. Important landmarks on the glass pipette include Point A, the 'larger opening' of the pipette; Point C, the 'body of pipette'; Point B, 'the indented transition point' between Point A and C; Point E, the 'narrow opening' of the pipette; and Point D, the 'narrowing transition point' between C and E. B. Flame seal ratings include: 1) 'good': clearly visible button sitting nicely on top the fully sealed end A; 2) 'average': button is a larger offshoot that may be jagged in shape; and 3) 'bad' no button, and the integrity of the seal is not clear.

During the initial flame seal, the heat from the torch may burn some of the organic material in a sample (e.g. protein in a blood plasma sample), especially if sample was directly inserted rather than using microcapillaries. This burning could occur because when the sample was inserted via micropipette some of the sample dripped or smeared when pulling the pipette tip out through the larger opening, or because when balancing the pipette horizontally, some of the sample drifted too far toward the indented transition point. Burns may be minimal (small dark spot occurs near the large

Table 2. Comparison between analyses of in-house flame sealed United States Geological Survey water standard, USGS48 (n = 13), and published data for this standard. In-house analyses were completed over a four-month span

Study	δ ¹⁷ Ο (‰)	δ ¹⁸ Ο (‰)	δ ² H (‰)	d-excess (‰)	Δ ¹⁷ O (per meg)			
This study	-1.15 (± 0.03)	-2.24 (± 0.05)	-2.43 (± 0.35)	15.44 (± 0.47)	33 (± 4)			
Aron et al. [39]	-1.10 (± 0.20)	N/A	N/A	N/A	31 (± 6)			
Berman et al. [52]	-1.15 (± 0.01)	$-2.23 (\pm 0.02)$	N/A	N/A	26 (± 3)			
USGS Published Values [56]	N/A	-2.22 (± 0.01)	$-2.00 (\pm 0.4)$	15.76*	N/A			

^aCalculated from published values and therefore does not have an accompanying standard deviation.

opening), mild (small dark smudging occurs), moderate (large dark smudging occurs), or severe (nearly all of the area past the indented transition point is dark – see Figure 2). Moderate to severe burning has a higher chance of altering the isotopic composition of the sample because water vapor is generated as a byproduct of the combustion. In addition, if the sample drifts too close to the indented transition point of the glass pipette but burning does not occur, evaporation and condensation still may occur during flame sealing, which can be indicated by the sudden appearance of water vapor on the glass; these processes can also affect the isotopic composition by causing fractionation. After the glass has been sealed, promptly check the warmth of the glass pipette immediately adjacent to the indented transition point, toward the body of the pipette; this section should be almost cool to the touch even immediately after sealing. If this

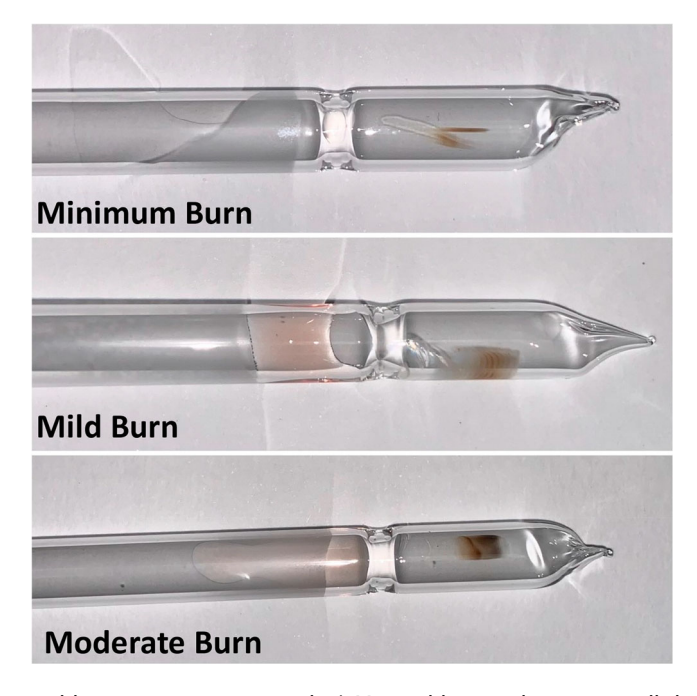


Figure 2. Flame seal burn rating system used: 1) Minimal burn indicates a small dark spot occurred near the large opening; 2) mild burn indicates a small dark smudging occurred; 3) moderate burn indicates a large dark smudging occurred; 4) Severe burn indicates nearly all of the area past the indented transition point is dark (not pictured).

section is warm or hot, evaporation likely occurred. Evaporation can be estimated as minimal (glass was warm to the touch), mild (hot to the touch but no visible water vapor), moderate (hot to the touch and some water vapor visible), or severe (hot to the touch and lots of water vapor visible; Figure 3). Noting potential evaporation, burns, and the appearance of the seal at this point will provide very useful information when interpreting your isotope measurements.

Burning and evaporation are only briefly mentioned by Nagy [22], likely because using microcapillaries reduces their occurrence. However, the tradeoff includes elevated risk of the microcapillaries shattering or sample remaining trapped in the microcapillaries. Over the past three years we have distilled > 1000 samples and found that the likelihood of distillation failure nearly doubles when using microcapillaries. While certain studies require the use of microcapillaries, we recommend that when possible, samples collected in microcapillaries be transferred to vials to facilitate simpler distillation.

After the first seal has been completed, a vacuum pump and LN_2 or dry ice are required for the next step. A container of LN_2 or dry ice should be securely angled with an opening that is easily accessible (Figure 4A). After gathering the necessary materials, the narrow opening of the glass pipette must be connected to a vacuum pump (e.g. using a series of tubing connections). Before turning on the vacuum pump, the newly sealed larger opening of the glass pipette is dipped into the LN_2 or placed on the dry ice. Always confirm that the larger opening is fully sealed before proceeding to submerge the pipette in LN_2 by tapping on the body of the pipette to observe if any sample escapes from the seal completed at the larger opening. As Nagy [22] recommends, the narrow opening of the pipette should already be attached to the vacuum line before dipping the end of the sealed larger opening into the LN_2 . The sealed larger opening of the glass pipette is then dipped into the LN_2 long enough to freeze the sample solid. Do not leave the glass pipette in the LN_2 longer than necessary because this increases the

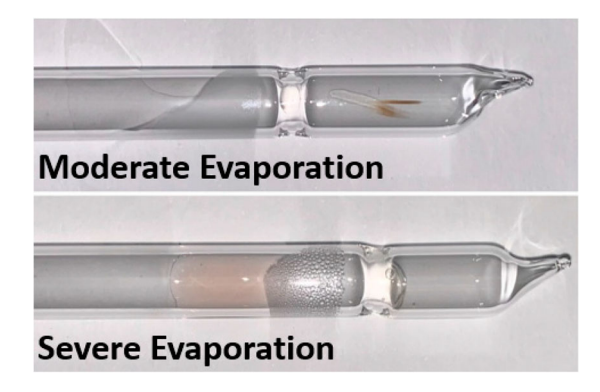


Figure 3. Flame seal evaporation rating system: 1) minimal evaporation indicates the glass beyond the indented transition point (see Figure 1A Point B) is warm to the touch but there is no visible water vapor (not pictured); 2) mild evaporation indicates that the glass beyond the indented transition point is hot to the touch but there is no visible water vapor (not pictured); 3) moderate evaporation indicates that the glass beyond the indented transition point is hot to the touch and some water vapor is visible; and 4) Severe evaporation indicates the glass beyond the indented transition point is hot to the touch and lots of water vapor is visible. If severe evaporation occurs, we recommend abandoning that distillation attempt at that point.

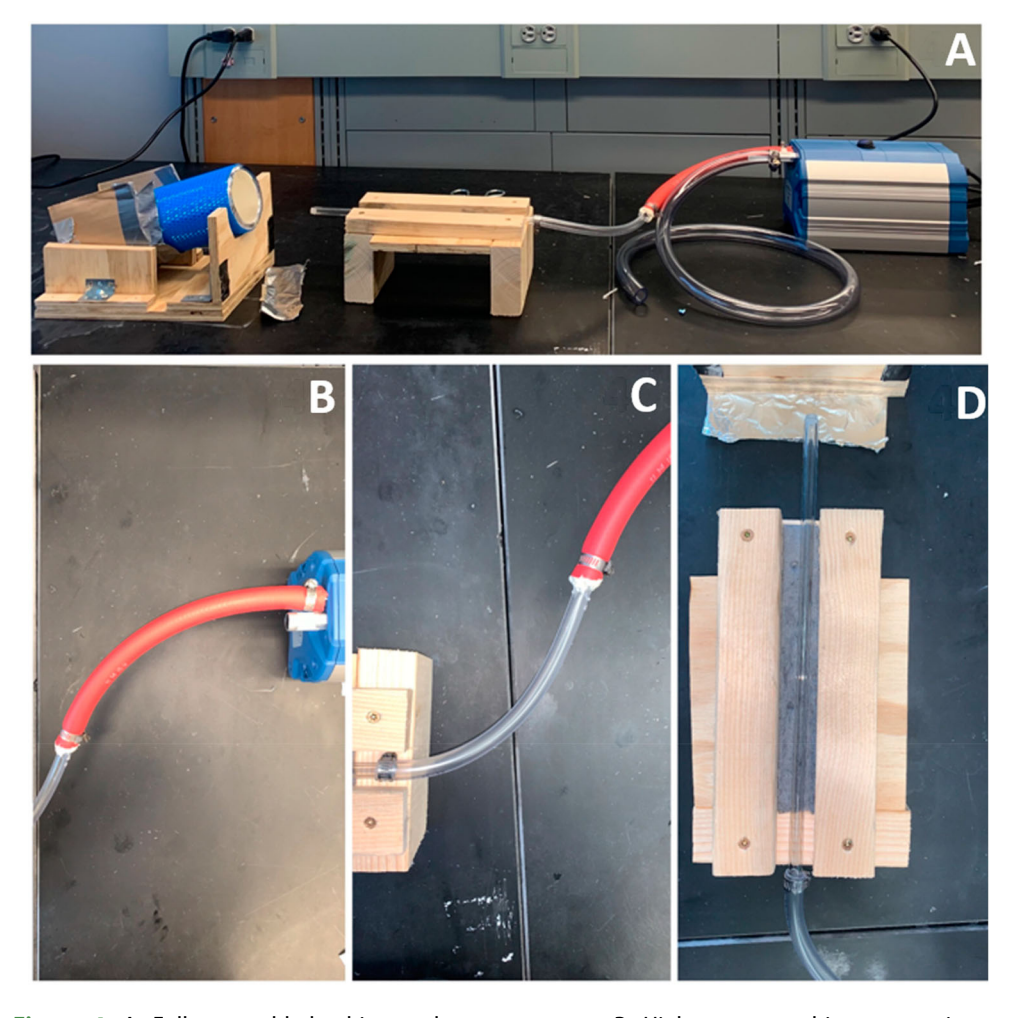


Figure 4. A. Fully assembled tubing and vacuum pump. B. High-pressure tubing connecting to vacuum pump (e.g. Vacuubrand ME1). C. Clear, pliable, plastic tubing connecting to both the highpressure tubing and the glass tubing. D. Glass tubing connected to both the plastic tubing and the pipette used for distillation. A small rubber stopper is attached at the end of the glass tubing opposite of the end connected to the plastic tubing.

likelihood of the glass cracking, which is particularly important if using microcapillary tubes because the sections of tubes may shatter.

Once the sample is frozen, remove the glass pipette from the LN₂ and position it as a bridge between the LN₂ container and the vacuum line tubing (Figure 5A). Turn the vacuum pump on and listen carefully for leaks in the vacuum line or glass breaking, as this may be audible. Quickly examine the narrow end of the glass pipette: a proper vacuum seal will cause the condensation formed from the LN2 to visibly retreat toward the narrowing transition point of the glass pipette (see Figure 5B). If the condensation does not retreat toward the narrowing transition point, the sealed larger opening likely shattered or there may be a vacuum leak. If the condensation does retreat, grasp the narrowing transition point with the forceps and create a flame seal close to the narrow



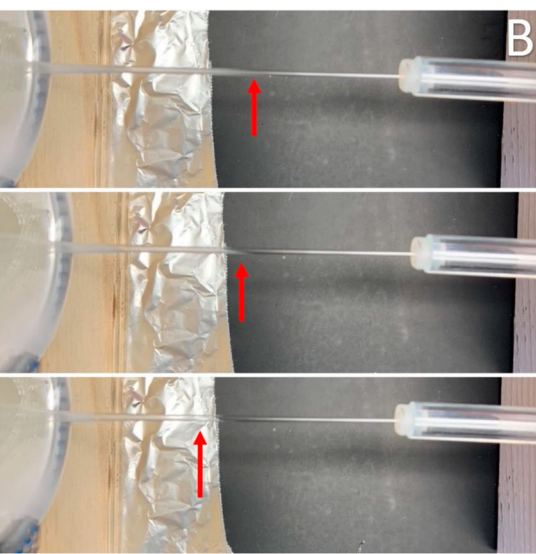


Figure 5. A. Pipette balancing on the lip of the dewar prior to vacuum sealing. B. The narrow end of the glass pipette after turning on the vacuum pump. Starting the vacuum pump should result in the condensation formed from the LN_2 visibly retreating toward the narrowing transition point of the glass pipette (see Figure 1A Point D). This retreat implies a proper vacuum seal. If the condensation does not retreat toward the narrowing transition point, the initially sealed opening (see Figure 1A Point A) likely shattered or there may be a vacuum leak.

opening, while avoiding damage to the tubing connecting to the vacuum pump. A pipette that is now fully sealed at both ends should be the product at this stage, along with a small discardable piece remaining from the most recent flame seal. When discarding this small piece, observe carefully to ensure that the piece was attached firmly to the tubing. When the piece is removed from the tubing, a small release of air should be audible, signifying that the connection of the tubing allowed for a proper vacuum seal.

Once this second flame seal has been completed, the glass pipette should be transferred to a slide warmer that is set to 50-60 °C. Label the pipette because all samples look alike at this stage. Importantly, the narrow end of the pipette should extend 6-8 cm (depending on how much glass was removed during the second seal) beyond the edge of the slide warmer (Figure 6A), allowing the gradual movement of water from the sealed larger opening to the sealed narrow opening. Monitor the sample and move the sealed narrow opening further beyond the edge if the water becomes clogged at the narrowing transition point, or if bubbles appear to be forming between the narrowing transition point and the sealed narrow opening. Aluminum foil can also be placed over the slide warmer to consolidate heat and speed condensation (Figure 6B). Typically, condensation is complete within 6–8 h. However, some samples require \geq 24 h, potentially reflecting cracking of the glass pipette, excessive or uneven heat on the slide warmer, or incorrect positioning of the pipette. In some cases, tapping or rubbing on the narrow end until the water properly transitions to the sealed narrow opening can help, but this may also cause water to return to the narrowing transition point or the body of the pipette.

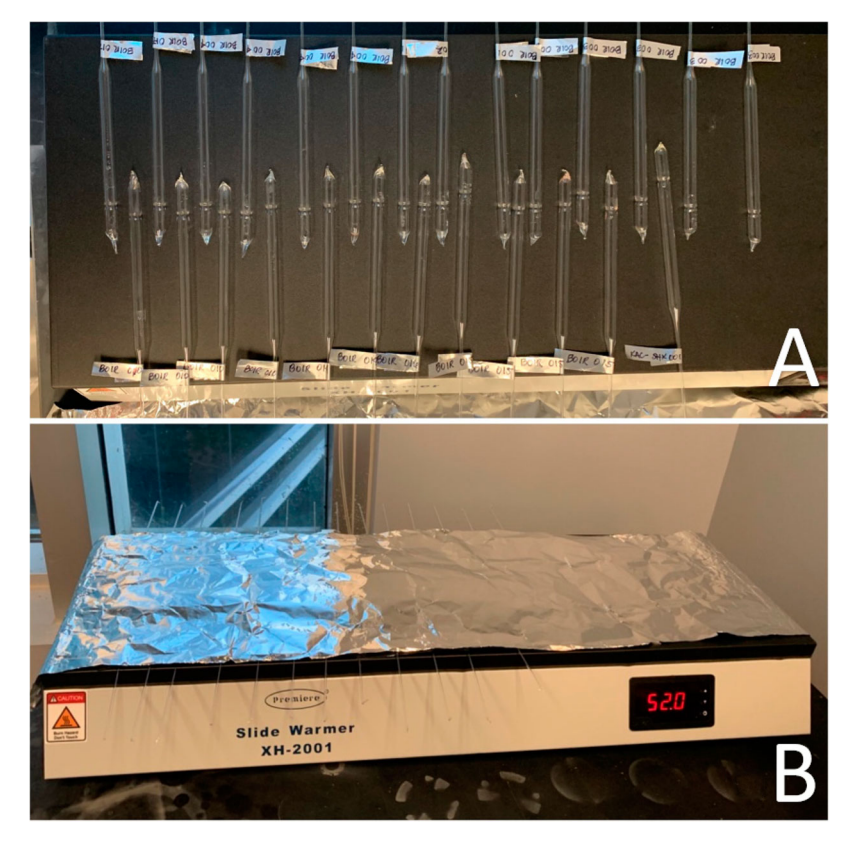


Figure 6. A. Slide warmer with pipettes positioned so the narrow end is slightly hanging off the side while the larger end is positioned within the heated area to allow condensation to occur. Each pipette is labeled and wrapped with aluminum foil for easy identification later. B. An aluminum foil cover can be placed over the slide warmer after all pipettes are positioned to help trap heat and allow for proper condensation of sample from the larger end to the narrow end.

Once the distilled water has condensed at the sealed narrow opening, a final flame seal completes the distillation process. This final seal is quick and should not require forceps. Set up the torch and lock the flame as described previously, then grasp the pipette with both hands, one hand at body of the pipette and the other at the sealed narrow opening. Slowly bring the narrow point of the glass pipette that is furthest from the distilled water toward the flame. This should be around the midpoint between the narrowing transition point and the sealed narrow opening but may be closer to the narrowing transition point if air gaps are present in the water that has accumulated at the sealed narrow opening. After bringing the glass pipette into the flame, quickly rotate the pipette for a few seconds and then pull apart the two ends to separate the completed sample from the remaining larger end. The remaining distilled sample should resemble a sealed microcapillary tube.

During this last flame seal, burning may occur if the distillation was incomplete or if sample drifted too far toward the narrowing transition point and the sealed narrow opening during the initial seal. Evaporation can also occur if the final seal is too close to where the water has gathered between the narrowing transition point and the sealed narrow opening. If significant evaporation occurs, some of the water may transfer

back into the larger end of the pipette that is separated from the completed sample. This 'leftover water' presents the most significant risk to the integrity of the sample. A large amount of leftover water can be caused by evaporation of sample during the final flame seal, leaving sample integrity as questionable at best. However, water can also be trapped at the sealed larger opening if the distillation did not progress correctly (e.g. some or all of the body water remained in the sealed larger opening) or if the glass pipette was removed too early from the slide warmer before all the water could transition toward the sealed narrow opening. This trapped water can be hard to observe, so it is critical to check the remaining larger end of the pipette that was separated from the completed sample before it is discarded.

We highly recommend taking detailed notes at all stages of the entire distillation process. This includes noting the quality of the three flame seals, evaporation, burning, water leftover, and initial sample volume. We also recommend completing multiple distillations per sample when possible, as a quality-control check for consistency among distillations. Logging detailed records is highly useful for interpreting variation among multiple distillations from a single sample, or for determining the reliability of single distillations.

To quantify the importance of the different quality-control checks that can be recorded during distillation, we kept detailed notes for the processing of 457 samples of blood plasma from three different species (northern elephant seals [Mirounga angustirostris], gemsbok [Oryx gazella], and Rocky Mountain mule deer [Odocoileus hemionus hemionus]). We graded the success of each distillation on a three-point scale, based on the similarity of the subsequent measurement to the mean value of all distillations for the sample: a grade of 3 = within 0.1 % for δ^{17} O, 0.3 % for δ^{18} O, and 15 per meg for Δ^{17} O; 2 = within 0.25, 0.5 ‰, and 30 per meg, respectively; and 1 = exceeding the thresholds defined for 2. We also graded the quality-control steps for each distillation: each of the three flame seals received a grade (3 = good; 2 = average; 1 = bad), as did the status of the evaporation (3 = none/minimal; 2 = mild; 1 = moderate/severe), burning (3 = none/minimal; 2 = mild; 1 = moderate/severe), and amount of leftover water (3 = none; 2 = some; 3 = substantial). In a Spearman's correlation coefficients test, the distillation success grade positively correlated with grades for the final flame seal ($r_s = 0.174$; p < 0.001) and for avoiding leftover water ($r_s = 0.217$; p < 0.001; for details of all statistical analyses, please see S1 and Table S1). In a second analysis, avoiding leftover water positively correlated with grades for avoiding burning ($r_s = 0.129$; p = 0.006) and for avoiding evaporation $(r_s = 0.406; p < 0.001)$. In other words, burning and evaporation during the final flame seal did not correlate with distillation success, but they remained indirect threats to sample integrity because they increased the likelihood of leftover water.

We have included an example dataset of 38 plasma samples from mule deer to demonstrate achievable precision, both within and across individuals (see S2; biological interpretation of these data will occur in future publications). Each plasma sample was distilled multiple times to generate a compiled mean average, standard deviation, and standard error for the sample. A total of 172 distillations were included in this dataset (average of 4.5 distillations per sample). We then averaged each calculated standard deviation for the distillation of each individual sample to determine an overall precision for the dataset. The overall precision obtained for this dataset was approximately $\pm 0.06 \%$ for δ^{17} O, \pm 0.125 % for δ^{18} O, \pm 0.825 % for δ^{2} H, \pm 0.80 % for d-excess, and \pm 7 per meg for Δ^{17} O.



4. Analyzing distilled animal body water samples via cavity ring-down spectroscopy

IRMS has been the primary option for analyzing distilled animal body water samples because few alternatives with comparable accuracy and precision existed. Recently, the availability of more affordable CRDS and OA-ICOS instruments alternatives have shifted these instruments to the forefront of oxygen and hydrogen SIA in water samples [23,24,26,36]. Current CRDS and OA-ICOS instruments provide data comparable to IRMS without requiring chemical sample preparation [39], and often in a fraction of the time [23,24]. Here, we focus on CRDS analysis using a Picarro L2140-i.

The end product of distillation is a body water sample, potentially as small as \sim 35 μ L. Analyzing such small volumes using an autosampler requires the use of autosampler vial inserts (e.g. Thermo Scientific #C4010-629L). To transfer the sample into an insert, crack open both ends of the sealed makeshift microcapillary tube by using a sharpening stone then connect the smaller end of the glass tube to a microcapillary bulb or a syringe barrel and push the sample into the insert. Cap the vial and tap its sides until the sample settles at the bottom. Up to \sim 5 μL of sample may coat the sides of the insert, a potentially considerable loss, so careful sample transfer is critical. In our experience, the Picarro L2140-i requires \sim 10 μ L of sample at the bottom of the insert to provide enough depth for the syringe to gather sample for a proper injection; smaller volumes may result in a 'dry injection' with no data (Figure S1).

While 10 µL is sufficient for a single injection, multiple injections are necessary to produce reliable data. Instruments typically require $\sim 1.5 \, \mu L$ per injection, thus five injections would likely require > 17.5 µL when using a vial insert. Users also need to account for discarding a variable number of initial injections because of instrument memory effects, in which the isotope value of previous injections influences the current injection. Accounting for the memory effect is a major hurdle in CRDS and OA-ICOS analyses [23,24,47]. A recent study suggested that ≥ 50 injections on a Picarro L2140-i can be required before δ^{17} O and δ^{18} O measurements of a single sample become reliable enough to calculate Δ^{17} O [47]. As 50 injections requires \sim 7.5 h when in high-precision analysis mode (as opposed to quicker analysis modes like high throughput), the need for so many injections eliminates the speed advantage over IRMS analyses [23,24,39]. The solution to this dilemma is an appropriately designed 'analysis run', which is the sequence of standards and unknown samples that will be analyzed in a designated timeframe.

Within an analysis run the memory effect is minimized with 'conditioning vials' that have a similar δ^{17} O or δ^{18} O as the sample that will be measured next [36]. It is important to prepare conditioning vials that span potential isotope values [36], which can be estimated using pilot measurements or contextual data such as isoscapes (i.e. maps of δ^{17} O, δ^{18} O, and δ^{2} H for precipitation or tap water; [48]). We have made conditioning vials with tap water from different regions and with different brands of bottled water, sourced from locations with unique and consistent δ^{18} O values (e.g. Kona Deep or Icelandic Glacial; [36,49]).

Analysis runs should also include control vials, serving both as conditioning vials and as quality-control checks. Measurements from control vials can be compared across analytical runs, and to published values. Control vials shared between labs can also add a layer of verification through interlaboratory comparison. Finally, analysis runs also include standards and unknown samples. We typically use three in-house standards in each analysis run, and we calibrate those in-house standards against internationally accepted standards (e.g. USGS46 [United States Geological Survey] or VSMOW2 [Vienna Standard Mean Ocean Water]; see below) several times per year. All standards, control vials, and unknown samples should be carefully stored to avoid fractionation.

Instrument maintenance also has the potential to influence measurements. For example, the Picarro L2140-i requires that the injection port septa be changed every 250–300 injections, and isotope values generally take \sim 10 injections to stabilize afterwards [47]. Septa changes during conditioning vial measurements minimize this disruption. Similarly, autosampler syringes and compressed gas tanks require regular replacement (every 1-3 months for both in our experience), Importantly, syringe and gas tank replacements can cause baseline shifts in measurements, and should be scheduled between standards runs. Lastly, long-term maintenance concerns include degradation of the particulate filter, the micro-combustion module (MCM) cartridge, and of the vaporizer tubing. The timeframe for replacing (MCM cartridge and filter) and needing to clean (vaporizer) these items will vary depending on the type of samples frequently analyzed (i.e. samples from herbivores and marine mammals likely contain more plant secondary compounds and salts, fouling filters and cartridges more guickly). For more details of routine maintenance, please see Hutchings and Konecky [50]. In addition, we have included our Picarro settings in Figure S2 and an example analysis run for reference (See Table 3).

5. Finalizing data

After an analysis run is complete, raw measurements of hydrogen and oxygen must be corrected to the VSMOW-SLAP scale (Standard Light Antarctic Precipitation; [51]). Note that VSMOW and SLAP are exhausted and have been replaced by VSMOW2 and SLAP2 and that other standards that have been validated on the VSMOW-SLAP scale (for δ^{18} O and δ^2 H) can be purchased, such as USGS water standards [39,52]. In our laboratory, we generally validate in-house and USGS standards against VSMOW-SLAP every ~ 2 months. In particular, we recommend validating in-house standards against international standards such as USGS immediately after syringe and gas tank changes.

After completing an analysis run, data must be cleaned. First, plot the raw values of the standards with injection number on the x-axis and the isotope value (e.g. δ^{18} O) on the y-axis. Raw values typically change unidirectionally then reach an obvious plateau, representing the waning memory effect (see Figure 7A). δ^2 H typically takes the longest to stabilize [47]. Discard the initial injections leading to the plateau, then calculate the mean and standard deviation of the remaining injections. Then, depending on the desired precision, measurements outside of a threshold (e.g. 0.75, 1, or 2 σ) can also be discarded to generate a final set of measurements (see Figure 7B). This cleaning process should be repeated for all standards utilized for the correction. Plots of δ^{17} O or δ^{18} O are suitable for determining which measurements to retain, but for some analyses plots of δ^2 H may be optimal because the additional stabilization time required may help eliminate the memory effect [47].

Once the data are cleaned, δ values (e.g. δ^{18} O) can then be corrected using equations derived from known versus measured values for standards by following two steps (both

Table 3. Example of an analysis run completed on the Picarro L2140-i. Three in-house standards (VA01, VA02, VA03) verified via internationally accepted water standards were incorporated throughout the run to enable correction of raw measurements. Injection total refers to the total number of injections as the run progresses while number of injections refers to the number of injections for that particular item, with more injections required for analyzed samples that vary greatly in δ^{18} O from the proceeding item. Autosampler job number refers to the order in which each item was listed for analysis. While a sample may have > 30 measurements, many of these measurements are removed due to the memory effect and only a select number of measurements remain for analysis.

Material being analyzed	Injection total	δ ¹⁸ Ο (‰)	Number of injections	Autosampler job number	Purpose
Conditioning vial	1–70	~ 0	70	1	Warm-up instrument
Conditioning vial	71–97	~ 4	27	2	Positioning δ ¹⁸ O for in-house standard analysis
In-house standard (VA01)	98–157	~ 8	60	3	First of three points for correction equation
Control vial	158-184	~ 4	27	4	Further validation of data
Control vial	185–211	~ −2	27	5	Further validation of data $\&$ positioning δ^{18} O for unknown samples
Distilled samples	212–361	???	150	6–17	Assessing isotope values of unknown biological samples
In-house standard (VA 02)	362–394	~ -4	33	18	Second of three points for correction equation
Control vial	395–437	~ -10	43	19	Further validation of data & positioning δ^{18} O for in-house standard
In-house standard (VA03)	438–470	~ -9	33	20	Third point for correction equation
Total Injections	470				
Estimated run time	~ 72	h			

steps are shown for δ^{18} O, but both are also applied to δ^{17} O): the determination of a 'stretching factor', followed by the generation of an 'offset value' [53,54]. First, a stretching factor is obtained by comparing the known difference between VSMOW and SLAP with the measured difference between VSMOW and SLAP:

$$\delta^{18}O_{\text{Stretching factor}} = (\delta^{18}O_{\text{VSMOW known}} - \delta^{18}O_{\text{SLAP known}})/(\delta^{18}O_{\text{VSMOW measured}} - \delta^{18}O_{\text{SLAP measured}})$$
(3)

Second, an offset value is calculated, to account for variation among laboratories in the measured difference between VSMOW or SLAP:

$$\delta^{18}O_{offset\ value} = \delta^{18}O_{VSMOW\ known} - (\delta^{18}O_{VSMOW\ measured} \cdot \delta^{18}O_{stretching\ factor})$$
 (4)

This offset value can be calculated using either VSMOW or SLAP [54]. Once an offset value and stretching factor have been determined, raw values can be corrected using the following equation:

$$\delta^{18}O_{corrected\ value} = \delta^{18}O_{stretching\ factor} \cdot \delta^{18}O_{raw\ value} + \delta^{18}O_{offset\ value}$$
 (5)

Equation (3) is essentially a slope-intercept equation (y = mx + b) that is then applied to all raw values [54]. Alternatively, a similar slope-intercept equation can be determined by linear regression with measured values as the independent variable and the known values as the dependent variable (typically using either two or three standards; [54]). Once δ^{17} O, δ^{18} O,

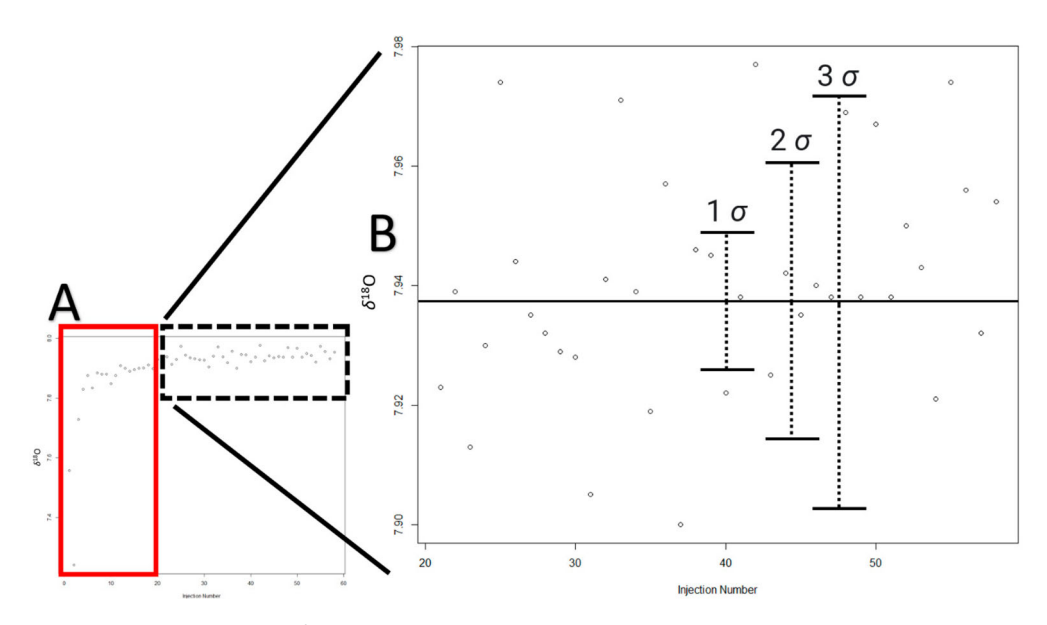


Figure 7. A. Example of δ^{18} O values (y-axis) and injection number (x-axis) of an in-house standard measured on a Picarro L2140-*i*. The solid red box highlights the first 20 injections, which include the adjustment period as values stabilize after previous measurements. This adjustment period can range from between 3–25 injections depending on the proximity of the values of the previous sample or standard that was measured. B. After removing measurements from the adjustment period, the range of δ^{18} O (y-axis) values becomes much smaller (as highlighted by zooming in on the dashed black box in A). At this point, a mean should be calculated for the raw δ^{18} O values (line dividing the plot) and a standard deviation as well. Depending on the goal of the analysis (e.g. Δ^{17} O or δ^{2} H analysis versus δ^{18} O analysis), the user should determine the appropriate number of standard deviations (e.g. 1, 2, 3 σ etc.) to use as a cutoff line, excluding measurements beyond this line.

and δ^2 H values are corrected, Δ^{17} O and d-excess can be calculated using these corrected values. As a quality control check when using three standards, corrections can be used to correct the measured values of standards themselves. For example, when measuring Δ^{17} O_{BW}, we expect that corrected standard values should agree with known standard values within (1) 0.01 ‰ for δ^{17} O; (2) 0.03 ‰ for δ^{18} O; and (3) 12 per meg for Δ^{17} O [39]. Other applications such as DLW measurements should not require such high precision.

Next, apply the obtained correction equations (i.e. δ^{17} O, δ^{18} O, and δ^{2} H) to the data obtained from the control samples. Corrected control samples tend to vary more thus we use the following thresholds when measuring Δ^{17} O_{BW}: (1) δ^{17} O should agree within 0.1 ‰ of our long-term average value; (2) δ^{18} O should agree within 0.3 ‰; (3) and Δ^{17} O should agree within 15 per meg. If the corrected values of the control samples fail to meet the desired thresholds, consider returning to the initial step of removing non-stabilized values from initial injections, revising the value selection, and obtaining a new correction equation. However, at that point, the integrity of the standards or the design of the analysis run may need to be questioned.

Finally, the correction equations can be applied to the unknown samples. Determining the number of non-stabilized values of initial injections to discard for an unknown sample is critical, and should be relatively uniform across unknown samples. Similar to the standard process, plot the corrected values and visually assess whether a plateau occurs (see Figure 7A). After removing the initial injections, calculate the mean and standard deviation of the remaining injections. Then, depending on the desired precision, measurements outside of a pre-determined threshold can also be discarded to generate a final set of measurements (see Figure 7B). Ideally, a sample is distilled multiple times and each distillation is measured during different analytical runs. Close agreement among the means for each distillation suggests that the distillation and measurement processes did not affect the isotope values. Typically, for samples, our goal is for mean values of individual distillations to be very similar to the grand mean across the distillations: within 0.1 % for δ^{17} O, 0.3 % for δ^{18} O, and 15 per meg for Δ^{17} O (see S2 for reference). Online supporting material includes our R and Python code for the correction process outlined above (see S3), Programs such as LIMS (Laboratory Information Management System) for Lasers can also be used [55].

6. Conclusion

Distilling body water samples for SIA analysis is an increasingly useful tool, and we hope that this manuscript supports wider adoption of this approach. Practitioners should stay up to date with new developments. Ongoing discussions in the scientific community include questions such as (1) whether two-point or three-point correction curves are more advantageous; (2) how many injections are required to produce reliable data when using CRDS or OA-ICOS; (3) how much variation is acceptable from each potential source (e.g. from the distillation process versus from instrument error); and (4) how to standardize data cleaning practices for constructing correction curves and determining final δ^{17} O, δ^{18} O, Δ^{17} O, δ^{2} H, and d-excess values. We believe these discussions, and widespread use of SIA analyses, will provide major benefits to ecology and animal biology.

Acknowledgements

We thank J. Ritter, C. Penix, W. Jensen, and A. Gaines for their data processing and contributions to the distillation process, and A.R. Gerson for contributing methodological support. We thank S. Newsome and Z. Sharp for insights regarding Δ^{17} O applications. We also thank S. Clayton for contributing data management support. Samples for this research were contributed via collaborations with: (1) D.P. Costa and R.R. Holser at the University of California, Santa Cruz (northern elephant seal samples were collected under protocols NMFS #19108 & 23188 and UCSC IACUC protocol Costd2009-1); (2) M. Ditmer at the Rocky Mountain Research Station (U.S. Forest Service – U.S. Department of Agriculture; Rocky Mountain mule deer samples were collected as part of routine sampling by the Utah Division of Wildlife Resources [UDWR] and all animal handling and sample collection were done under the direct supervision of a veterinarian within the UDWR). (3) G. Villegas and P. Morrow at the Environmental Division of the U.S. Army Garrison White Sands Missile Range, New Mexico (gemsbok samples were voluntarily collected post-mortem by hunters from culled carcasses, after regulated, routine harvest that is managed by White Sands Missile Range and the New Mexico Department of Game and Fish).

Data deposition

https://github.com/ZacharyTSteele/Automated Templates https://github.com/ZacharyTSteele/IEHS VideoS1 https://github.com/ZacharyTSteele/IEHS_Example_Dataset

Disclosure statement

No potential conflict of interest was reported by the author(s).

Funding

This work was supported by the National Science Foundation under grant IOS-1941853 (JPW); T & E, Inc. Conservation Grant (ZTS); a Virginia Space Grant Consortium Graduate Research STEM Fellowship (ZTS); and Old Dominion University.

Data availability statement

Data related to post-processing of isotope analyses in this manuscript is included in the listed Github repository. An example dataset is provided as well in the listed Github repository to demonstrate achievable precision with this method. All other data is available upon request from the corresponding author (ZTS).

References

- [1] Newsome SD, Martinez del Rio C, Bearhop S, et al. A niche for isotopic ecology. Front Ecol Environ. 2007;5:429-436. doi:10.1890/1540-9295(2007)5[429:ANFIE]2.0.CO;2
- [2] Cucherousset J, Villéger S. Quantifying the multiple facets of isotopic diversity: new metrics for stable isotope ecology. Ecol Indic. 2015;56:152-160. doi:10.1016/j.ecolind.2015.03.032
- [3] Whiteman JP, Elliott Smith EA, Besser AC, et al. A guide to using compound-specific stable isotope analysis to study the fates of molecules in organisms and ecosystems. Diversity (Basel). 2019;11:8.
- [4] McCue MD, Javal M, Clusella-Trullaset S, et al. Using stable isotope analysis to answer fundamental questions in invasion ecology: Progress and prospects. Methods Ecol Evol. 2020;11:196-214. doi:10.1111/2041-210X.13327
- [5] Bongiorni L, Fiorentino F, Auriemma R, et al. Food web of a confined and anthropogenically affected coastal basin (the Mar Piccolo of Taranto) revealed by carbon and nitrogen stable isotopes analyses. Environ Sci Pollut Res. 2016;23:12725-12738. doi:10.1007/s11356-015-5380-z
- [6] Tawa A, Ishihara T, Uematsu Y, et al. Evidence of westward transoceanic migration of Pacific bluefin tuna in the Sea of Japan based on stable isotope analysis. Mar Biol. 2017;164:94), doi:10.1007/s00227-017-3127-8
- [7] Rofes J, Garcia-Ibaibarriaga N, Aguirre M, et al. Combining small-vertebrate, marine and stableisotope data to reconstruct past environments. Sci Rep. 2015;5:14219), doi:10.1038/srep14219
- [8] Vander Zanden HB, Soto DX, Bowen GJ, et al. Expanding the isotopic toolbox: applications of hydrogen and oxygen stable isotope ratios to food web studies. Front Ecol Evol. 2016;4:20), doi:10.3389/fevo.2016.00020
- [9] Whiteman JP, Sharp ZD, Gerson AR, et al. Relating Δ^{17} O values of animal body water to exogenous water inputs and metabolism. BioScience. 2019;69:658-668. doi:10.1093/biosci/ biz055
- [10] Andrews FM, Nadeau JA, Saabye L, et al. Measurement of total body water content in horses, using deuterium oxide dilution. Am J Vet Res. 1997;58:1060-1064. doi:10.2460/ajvr.1997.58.10. 1060
- [11] Speakman JR. Doubly labelled water: theory and practice. New York (NY): Springer Scientific Publishers; 1997.
- [12] Bryant JD, Froelich PN. A model of oxygen isotope fractionation in body water of large mammals. Geochim Cosmochim Acta. 1995;59:4523-4537. doi:10.1016/0016-7037(95)00250-4
- [13] Kohn MJ. Predicting animal δ^{18} O: accounting for diet and physiological adaptation. Geochim Cosmochim Acta. 1996;60:4811–4829. doi:10.1016/S0016-7037(96)00240-2



- [14] Pack A, Gehler A, Süssenberger A. Exploring the usability of isotopically anomalous oxygen in bones and teeth as paleo-CO₂-barometer. Geochim Cosmochim Acta. 2013;102:306-317. doi:10.1016/j.gca.2012.10.017
- [15] Sabat P, Newsome SD, Pinochet S, et al. Triple oxygen isotope measurements (Δ'^{17} O) of body water reflect water intake, metabolism, and δ^{18} O of ingested water in passerines. Front Physiol. 2021;12:710026), doi:10.3389/fphys.2021.710026
- [16] Fancy SG, Blanchard JM, Holleman DF, et al. Validation of doubly labeled water method using a ruminant. Am J Physiol Regul Integr Comp Physiol. 1986;251:R143-R149. doi:10.1152/ajpregu. 1986.251.1.R143
- [17] Hill RW, Wyse GA, Anderson M. Animal physiology. Sunderland (MA): Sinauer Associates; 2008.
- [18] Nguyen MK, Ornekian V, Butch AW, et al. A new method for determining plasma water content: application in pseudohyponatremia. Am J Physiol Renal Physiol. 2007;292:F1652-F1656. doi:10.1152/ajprenal.00493.2006
- [19] Murray IW, Fuller A, Lease HM, et al. The actively foraging desert lizard *Pedioplanis husabensis* (Husab Sand Lizard) behaviorally optimizes its energetic economy. Can J Zool. 2014;92:905-913. doi:10.1139/cjz-2014-0086
- [20] Smit B, Woodborne S, Wolf BO, et al. Differences in the use of surface water resources by desert birds are revealed using isotopic tracers. Auk. 2019;136:uky005), doi:10.1093/auk/uky005
- [21] Wood RA, Nagy KA, MacDonald NS, et al. Determination of oxygen-18 in water contained in biological samples by charged particle activation. Anal Chem. 1975;47:646-650. doi:10.1021/ ac60354a038
- [22] Nagy KA. The doubly labeled water (³HH¹⁸O) method: A guide to its use. Los Angeles (CA): Laboratory of Biomedical and Environmental Sciences, University of California; UCLA Publication; No.12-1417; 1983.
- [23] Thorsen T, Shriver T, Racine N, et al. Doubly labeled water analysis using cavity ring-down spectroscopy. Rapid Commun Mass Spectrom. 2011;25:3-8. doi:10.1002/rcm.4795
- [24] Melanson EL, Swibas T, Kohrt WM, et al. Validation of the doubly labeled water method using off-axis integrated cavity output spectroscopy and isotope ratio mass spectrometry. Am J Physiol Endocrinol Metab. 2018;314:E124-E130. doi:10.1152/ajpendo.00241.2017
- [25] Barkan E, Luz B. Diffusivity fractionations of H₂¹⁶O/H₂¹⁷O and H₂¹⁶O/H₂¹⁸O in air and their implications for isotope hydrology. Rapid Commun Mass Spectrom. 2007;21:2999-3005. doi:10. 1002/rcm.3180
- [26] Steig EJ, Gkinis V, Schauer AJ, et al. Calibrated high-precision ¹⁷O-excess measurements using cavity ring-down spectroscopy with laser-current-tuned cavity resonance. Atmos Meas Tech. 2014;7:2421-2435. doi:10.5194/amt-7-2421-2014
- [27] Clayton RN, Grossman L, Mayeda TK. A component of primitive nuclear composition in carbonaceous meteorites. Science. 1973;182:485-488. doi:10.1126/science.182.4111.485
- [28] Luz B, Barkan E, Bender m, et al. Triple-isotope composition of atmospheric oxygen as a tracer of biosphere productivity. Nature. 1999;400:547-550. doi:10.1038/22987
- [29] Thiemens MH. Mass-independent isotope effects in planetary atmospheres and the early Solar System. Science. 1999;283:341–345. doi:10.1126/science.283.5400.341
- [30] Bindeman IN, Eiler JM, Wing BA, et al. Rare sulfur and triple oxygen isotope geochemistry of volcanogenic sulfate aerosols. Geochim Cosmochim Acta. 2007;71:2326-2343. doi:10.1016/j. gca.2007.01.026
- [31] Lehmann SB, Levin NE, Passey BH, et al. Triple oxygen isotope distribution in modern mammal teeth and potential geologic applications. Geochim Cosmochim Acta. 2022;331:105-122. doi:10.1016/j.gca.2022.04.033
- [32] Hu H, Passey BH, Lehmann SB, et al. Modeling and interpreting triple oxygen isotope variations in vertebrates, with implications for paleoclimate and paleoecology. Chem Geol. 2023;642:121812), doi:10.1016/j.chemgeo.2023.121812
- [33] Feng D, Tütken T, Löffler N, et al. Isotopically anomalous metabolic oxygen in marine vertebrates as physiology and atmospheric proxy. Geochim Cosmochim Acta. 2022;328:85-102. doi:10.1016/j.gca.2022.05.008



- [34] Navarrete L, Lübcker N, Alvarez F, et al. A multi-isotope approach reveals seasonal variation in the reliance on marine resources, production of metabolic water, and ingestion of seawater by two species of coastal passerine to maintain water balance. Front Ecol Evol. 2023;11:1120271), doi:10.3389/fevo.2023.1120271
- [35] Wostbrock JA, Cano EJ, Sharp ZD. An internally consistent triple oxygen isotope calibration of standards for silicates, carbonates and air relative to VSMOW2 and SLAP2. Chem Geol. 2020;533:119432), doi:10.1016/j.chemgeo.2019.119432
- [36] Schauer AJ, Schoenemann SW, Steig EJ. Routine high-precision analysis of triple water-isotope ratios using cavity ring-down spectroscopy. Rapid Commun Mass Spectrom. 2016;30:2059-2069. doi:10.1002/rcm.7682
- [37] Landais A, Barkan E, Luz B. Record of δ^{18} O and δ^{17} O-excess in ice from Vostok Antarctica during the last 150,000 years. Geophys Res Lett. 2008;35:L02709.
- [38] Landais A, Ekaykin A, Barkan E, et al. Seasonal variations of ¹⁷O-excess and d-excess in snow precipitation at Vostok station, East Antarctica. J Glaciol. 2012;58:725-733. doi:10.3189/ 2012JoG11J237
- [39] Aron PG, Levin NE, Beverly EJ, et al. Triple oxygen isotopes in the water cycle. Chem Geol. 2021;565:120026), doi:10.1016/j.chemgeo.2020.120026
- [40] Li S, Levin NE, Soderberg K, et al. Triple oxygen isotope composition of leaf waters in Mpala, central Kenya. Earth Planet Sci Lett. 2017;468:38-50. doi:10.1016/j.epsl.2017.02.015
- [41] Landais A, Barkan E, Yakir D, et al. The triple isotopic composition of oxygen in leaf water. Geochim Cosmochim Acta. 2006;70:4105-4115. doi:10.1016/j.gca.2006.06.1545
- [42] Voigt C, Alexandre A, Reiter IM, et al. Examination of the parameters controlling the triple oxygen isotope composition of grass leaf water and phytoliths at a Mediterranean site: a model-data approach. Biogeosciences. 2023;20:2161-2187. doi:10.5194/bg-20-2161-2023
- [43] Kahmen A, Schefuß E, Sachse D. Leaf water deuterium enrichment shapes leaf wax n-alkane δD values of angiosperm plants I: Experimental evidence and mechanistic insights. Geochim Cosmochim Acta. 2013;111:39–49. doi:10.1016/j.gca.2012.09.003
- [44] Zhou Y, Grice K, Chikaraishi Y, et al. Temperature effect on leaf water deuterium enrichment and isotopic fractionation during leaf lipid biosynthesis: results from controlled growth of C_3 and C_4 land plants. Phytochemistry. 2011;72:207–213. doi:10.1016/j.phytochem.2010.10.
- [45] Newsome SD, Clementz MT, Koch PL. Using stable isotope biogeochemistry to study marine mammal ecology. Mar Mammal Sci. 2010;26:509-572.
- [46] Crowley BE. Stable isotope techniques and applications for primatologists. Int J Primatol. 2012;33:673-701. doi:10.1007/s10764-012-9582-7
- [47] Vallet-Coulomb C, Couapel M, Sonzogni C. Improving memory effect correction to achieve high-precision analysis of δ^{17} O, δ^{18} O, δ^{2} H, δ^{17} O-excess and d-excess in water using cavity ring-down laser spectroscopy. Rapid Commun Mass Spectrom. 2021;35:e9108), doi:10.1002/ rcm.9108
- [48] Li S, Levin NE, Chesson LA. Continental scale variation in ¹⁷O-excess of meteoric waters in the United States, Geochim Cosmochim Acta, 2015;164:110-126, doi:10.1016/j.gca.2015.04.047
- [49] Turk D, Bedard JM, Burt WJ, et al. Inorganic carbon in a high latitude estuary-fjord system in Canada's eastern Arctic. Estuar Coast Shelf Sci. 2016;178:137-147. doi:10.1016/j.ecss.2016.06. 006
- [50] Hutchings JA, Konecky BL. Optimization of a Picarro L2140-i cavity ring-down spectrometer for routine measurement of triple oxygen isotope ratios in meteoric waters. Atmos Meas Tech. 2023;16:1663-1682. doi:10.5194/amt-16-1663-2023
- [51] Schoenemann SW, Schauer AJ, Steig EJ. Measurement of SLAP2 and GISP δ^{17} O and proposed VSMOW-SLAP normalization for $\delta^{17}O$ and $^{17}O_{excess}$. Rapid Commun Mass Spectrom. 2013;27:582-590. doi:10.1002/rcm.6486
- [52] Berman ES, Levin NE, Landais A, et al. Measurement of δ^{18} O, δ^{17} O, and δ^{17} O-excess in water by off-axis integrated cavity output spectroscopy and isotope ratio mass spectrometry. Anal Chem. 2013;85:10392–10398. doi:10.1021/ac402366t
- [53] Sharp Z. Stable isotope geochemistry. Upper Saddle River (NJ): Pearson Prentice Hall; 2007.

- [54] Dunn PJH, Carter JF. Good practice guide for isotope ratio mass spectrometry. Bristol: Forensic Isotope Ratio Mass Spectrometry Network; 2018.
- [55] Usgs.gov. Reston, VA: United States Geological Survey; 2021. https://isotopes.usgs.gov/research/topics/lims.html#:~:text=What%20is%20%22LIMS%20for%20Light,thousand%20isotopic%20analyses%20per%20year.
- [56] Qi H, Coplen TB, Tarbox L, et al. USGS48 Puerto Rico precipitation a new isotopic reference material for δ^2 H and δ^{18} O measurements of water. Isotopes Environ Health Stud. 2014;50:442–447. doi:10.1080/10256016.2014.905555